# REPORT DOCUMENTATION PAGE

*Form Approved*
*OMB No. 0704-0188*



**PLEASE DO NOT RETURN YOUR FORM TO THE ABOVE ADDRESS.**

| 1. REPORT DATE *(DD-MM-YYYY)* | 2. REPORT TYPE | 3. DATES COVERED *(From - To)* |
|---|---|---|
| 08/13/2008 | Final Technical Report | 04/01/05-03/31/08 |

**4. TITLE AND SUBTITLE**

Utilization of GOES Rapid-Scan Wind Data for Tropical Cyclone Predictability Experiments

**5a. CONTRACT NUMBER**

**5b. GRANT NUMBER**

N00014-05-1-0494

**5c. PROGRAM ELEMENT NUMBER**

**6. AUTHOR(S)**

Christopher Velden

**5d. PROJECT NUMBER**

**5e. TASK NUMBER**

**5f. WORK UNIT NUMBER**

**7. PERFORMING ORGANIZATION NAME(S) AND ADDRESS(ES)**

Board of Regents of the University of Wisconsin System
21 N. Park Street, Suite 6401
Madison, WI 53715-1218

**8. PERFORMING ORGANIZATION REPORT NUMBER**

1400/NL92Final

**9. SPONSORING/MONITORING AGENCY NAME(S) AND ADDRESS(ES)**

Office of Naval Research
875 Randolph Street
Arlington, VA 22203-1995

**10. SPONSOR/MONITOR'S ACRONYM(S)**

**11. SPONSOR/MONITOR'S REPORT NUMBER(S)**

**12. DISTRIBUTION/AVAILABILITY STATEMENT**

Approved for Public Release; distribution is Unlimited

**13. SUPPLEMENTARY NOTES**

**14. ABSTRACT**

Experiments were performed testing the impact of modifying the assumed observation error for assimilating AMVs in the NRL Atmospheric Variational Data Assimilation System (NAVDAS). A first experiment changed the observation error for all Geostationary AMVs to be 1.5 times the model background error. This weighting is based on comparisons with an adjoint-based impact parameter. A second experiment kept the operational observation error settings for AMVs, but used experimental "expected error" quality indices on CIMSS-produced AMVS to reject AMVs that were indicated to have poor quality. A third experiment set the observation error of the CIMSS-produced AMVs equal to the expected error indices.

All three experiments produce forecast differences that are overall slightly positive in terms of forecast skill but with low statistical significance. The observation error ratio experiment produced Northern and Southern hemisphere extra-tropical 500-hPa height anomaly correlations that are slightly better than the control. The tropical 500-hPa height anomaly correlations are slightly

**15. SUBJECT TERMS**

| 16. SECURITY CLASSIFICATION OF: | | | 17. LIMITATION OF ABSTRACT | 18. NUMBER OF PAGES | 19a. NAME OF RESPONSIBLE PERSON |
|---|---|---|---|---|---|
| a. REPORT | b. ABSTRACT | c. THIS PAGE | | | John Roberts |
| U | U | U | SAR | 33 | 19b. TELEPHONE NUMBER *(Include area code)* 608-262-0985 |

# Utilization of GOES Satellite-Derived Wind Data for Tropical Cyclone Predictability Experiments

Christopher S. Velden
University of Wisconsin – CIMSS
1225 West Dayton St., room 229
Madison, WI 53706
Phone: 608 262 9168 fax: 608 262 5974 email: chrisv@ssec.wisc.edu

Award Number: N00014-05-1-0494
http://cimss.ssec.wisc.edu/tropic/tropex/index.html

## Final Report

### OVER-ARCHING GOAL

The overarching goal was to prepare geostationary satellite atmospheric motion vectors (AMV) for numerical model assimilation experiments and test for improvements in the NAVY global numerical model (NOGAPS) forecasts of tropical cyclones (TC) using targeting information provided by NRL-MRY. This was the primary motivation for this investigation.

### PRIMARY OBJECTIVE

Develop an AMV processing and data assimilation strategy to optimize positive impacts on NOGAPS forecasts of TC tracks and intensity.

### RESULTS: EXECUTIVE SUMMARY

Experiments were performed testing the impact of modifying the assumed observation error for assimilating AMVs in the NRL Atmospheric Variational Data Assimilation System (NAVDAS). A first experiment changed the observation error for all Geostationary AMVs to be 1.5 times the model background error. This weighting is based on comparisons with an adjoint-based impact parameter. A second experiment kept the operational observation error settings for AMVs, but used experimental "expected error" quality indices on CIMSS-produced AMVS to reject AMVs that were indicated to have poor quality. A third experiment set the observation error of the CIMSS-produced AMVs equal to the expected error indices.

All three experiments produce forecast differences that are overall slightly positive in terms of forecast skill but with low statistical significance. The observation error ratio experiment produced Northern and Southern hemisphere extra-tropical 500-hPa height anomaly correlations that are slightly better than the control. The tropical 500-hPa height anomaly correlations are slightly worse. For the expected error threshold experiment the forecast impact in the southern hemisphere is slightly better than the control while the northern hemisphere and tropical forecasts are slightly worse. The observation error/expected error experiment produced very little difference from the control.

## 1. Introduction

Geostationary satellite-derived Atmospheric Motion Vectors (AMVs) are used by numerical weather prediction (NWP) centers around the world. Although their forecast impacts are generally beneficial, the complexity of AMVs and their associated observation errors make them challenging to assimilate. The AMVs operationally assimilated in NAVDAS (the NRL Atmospheric Variational Data Assimilation System) are produced by the University of Wisconsin's Cooperative Institute for Meteorological Satellite Studies (CIMSS), the National Environmental Satellite Data and Information Service (NESDIS), the U.S. Air Force Weather Agency (AFWA), the European Meteorological Satellite Organization (EUMETSAT), and the Japan Meteorological Agency (JMA). AMVs valid within a six-hour time window around the NAVDAS analysis time are ingested for assimilation. To reduce the data volume, these AMVs are superobbed. AMVs from different sensors, satellites, and processing centers are all superobbed separately. Details of the superobbing scheme are presented in Pauley (2003).

AMVs have a large and beneficial impact on NOGAPS (Navy Operational Global Atmospheric Prediction System) forecast skill. For example, as described in Langland and Baker (2004), AMVs produce the second-largest reduction in NOGAPS 24-hr forecast error, following rawinsonde observations in the Northern Hemisphere and Advanced Microwave Sounding Unit (AMSU-A) observations in the Southern Hemisphere. Although, on average, their impact is beneficial (e.g., their assimilation reduces model forecast error), the impact of individual AMVs (and other types of observations) has a statistical distribution that includes both beneficial and non-beneficial forecast impacts. This distribution of impacts is due to our inability to exactly specify the

true errors of the observations and the background (model first-guess), which are combined in the data assimilation process to produce the analysis or initial conditions. If these errors can be more precisely tuned, the observations will have a greater beneficial impact on model forecast skill.

This report will describe three NOGAPS model forecast experiments in which we adjust the quality control and specified observation errors for AMV assimilation into NAVDAS. In Section 2 we use information from the observation impact procedure developed by Langland and Baker (2004). In Section 3, we use a newly available AMV quality indicator, referred to as the "expected error", and conduct two forecast impact experiments. The results of these three experiments are then summarized and followed by discussion and ideas for future efforts.

## 2. Adjoint-based Observation Impact Results

Langland and Baker (2004, LB04 hereafter) describe a procedure to estimate the impact of individual observations on a measure of short-range forecast error. This method is useful for determining which observations improve the forecast, and regional patterns in observation impacts on the forecast. The LB04 observation impact equation is:

$$\delta e_f^g = \left\langle (y - Hx_b), K^T \left[ \frac{\partial J^f}{\partial x_a} + \frac{\partial J^g}{\partial x_b} \right] \right\rangle \qquad (1)$$

where $y - Hx_b$ is the innovation (difference between the observation and the background, $\frac{\partial J^f}{\partial x_a}$ and $\frac{\partial J^g}{\partial x_b}$ are, respectively, the sensitivity of forecast errors on the analysis and background model trajectories, and $K^T$ is the transpose of the Kalman gain matrix represented by the data assimilation procedure. The quantity "$J$" is an energy-

weighted forecast error norm that includes temperatures, winds, moisture, and surface pressure from the surface to about 300 hPa. In these results, $f$ represents a 24-hour forecast. The $\langle\ \rangle$ brackets represent a scalar inner product. The observation impact $\delta e_f^g$ is an approximation of the increase or decrease in forecast error associated with the assimilation of observations. In this context, negative values of $\delta e_f^g$ imply a forecast error reduction, which is a "beneficial" impact. We can use $\delta e_f^g$ to represent the impact of all observations, or any arbitrary subset of observations. This adjoint-based method provides information about observation impact that is difficult or impossible to obtain from conventional data denial experiments.

Using the LB04 method, observation impact values were calculated for 0000 UTC analyses from 3–10 July 2007, and include all geostationary AMV data used in NAVDAS operations. Figure 1 and Figure 2 (top panels) shows the observation impact sum binned as a function of wind component (u or v) speed (Figure 1) and wind direction (Figure 2). The lower panels of each figure show the corresponding number of observations in each bin. These figures show that the total impact is fairly well correlated with the number of observations in each bin. Thus, there is no strong bias for lower or higher wind speeds, or winds from any particular direction to have larger impact on short-range forecast skill.

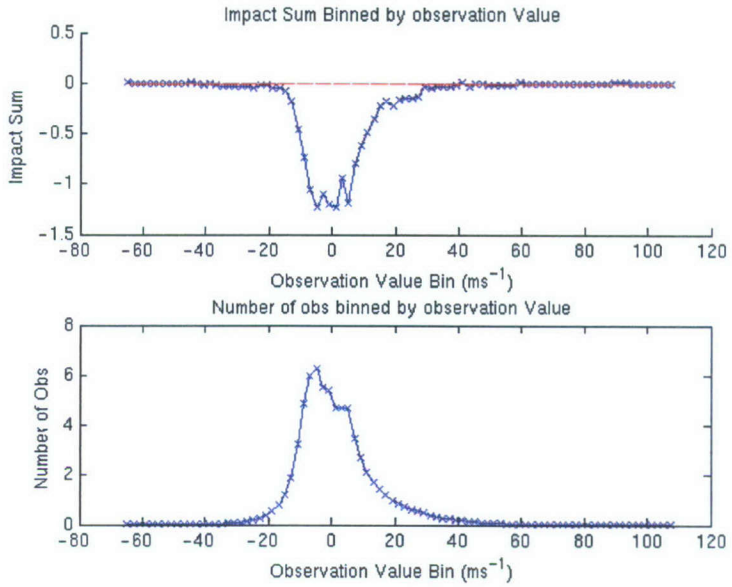


**Figure 1:** Observed AMV wind component value (m s$^{-1}$) vs. summed observation impact (top panel) and number of observations (lower panel).

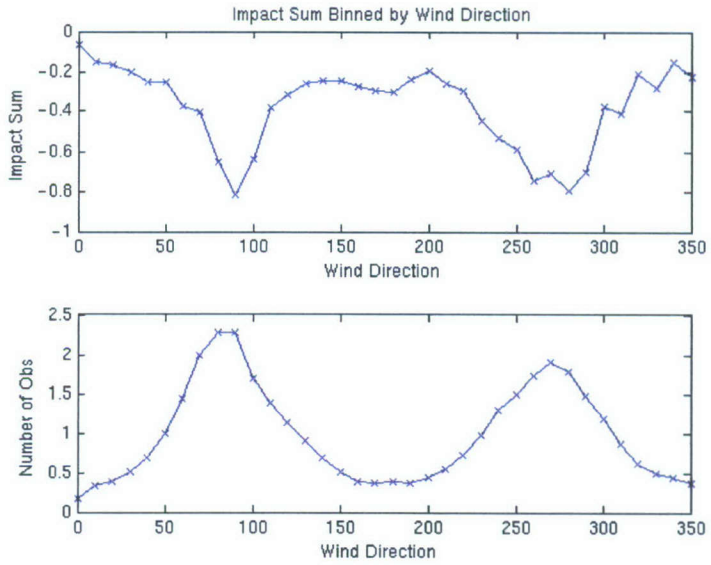


**Figure 2:** Observed AMV wind direction (degrees) vs. summed observation impact (top panel) and number observations (lower panel)

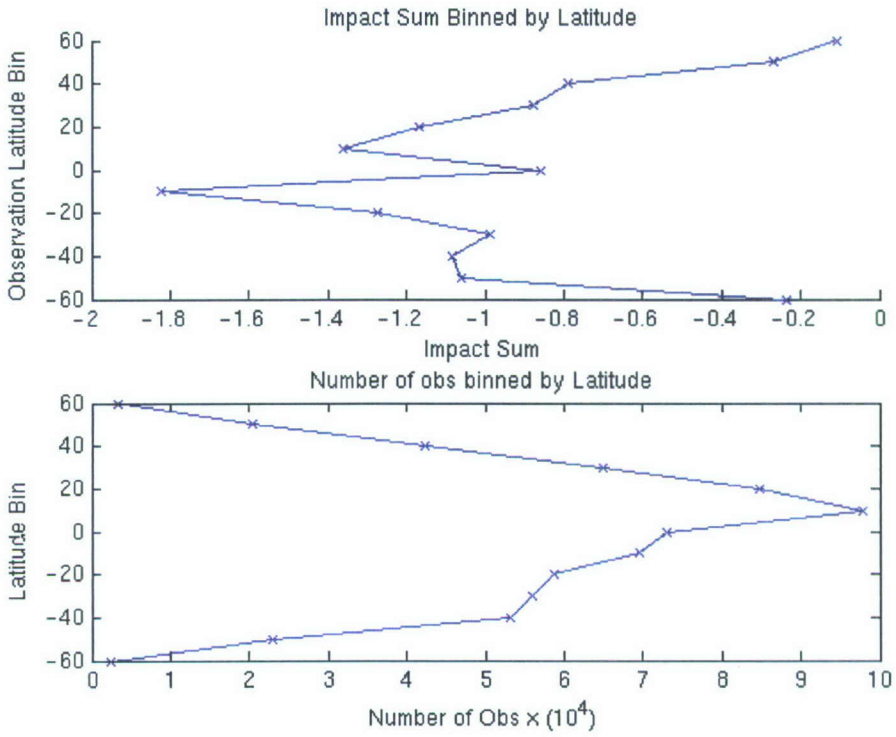


**Figure 3:** Observed AMV latitude (y-axis) vs. summed observation impact (top panel) and number of observations (lower panel). AMVs have the largest impact just south of the equator, although there are more observations just north of the equator. This may be explained by the larger number of other upper-air observations (e.g., radiosondes, aircraft observations) in the Northern Hemisphere that reduces somewhat the impact of AMVs.

In figures 3-5 we show AMV observation impact and observation counts as functions of, respectively, observation latitude, longitude, and pressure. Figure 3 illustrates that the maximum observation impact is near 10° S, with a secondary peak near 10° N latitude. Although the largest number of AMV observations is near 10° N, there are also more competing types of upper air observations (.e.g, radiosondes, aircraft) north of the equator, which reduces the total impact of the AMVs. Thus, the peak impact of AMV observations occurs just south of the equator, where AMVs contribute proportionately more to the analysis.

As a function of longitude (Figure 4), the observation impact is generally proportional to the number of observations, with a peak in the Atlantic basin, near 45° W. The large number of AMV observations here is probably caused by an overlap in coverage provided by GOES-E and Meteosat-9.

The plot of AMV impact as a function of pressure (Figure 5) shows several important features. The AMVs impact the forecast in two regions: in the lower troposphere near 850-hPa and near the level of the upper tropospheric jet streams near 400-hPa. The 850-hPa maximum is slightly above the level (900 hPa) where the number of lower tropospheric AMVs is largest, and the 400-hPa slightly below the level (300-hPa) where the number of upper tropospheric AMVs is largest. As AMV observation error is soley a function of pressure, this result suggests that the specification of observation and background errors in NAVDAS is not optimal at certain levels. Specifically, it appears that AMVs at 300-hPa and 900-hPa should have larger beneficial impact than is shown in Figure 6.

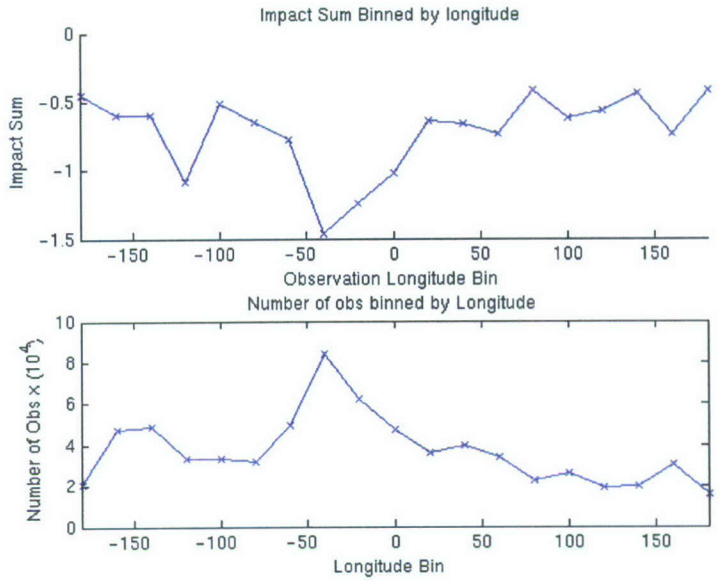


**Figure 4:** Observed AMV longitude vs. summed observation impact (top panel) and number of observations (lower panel).

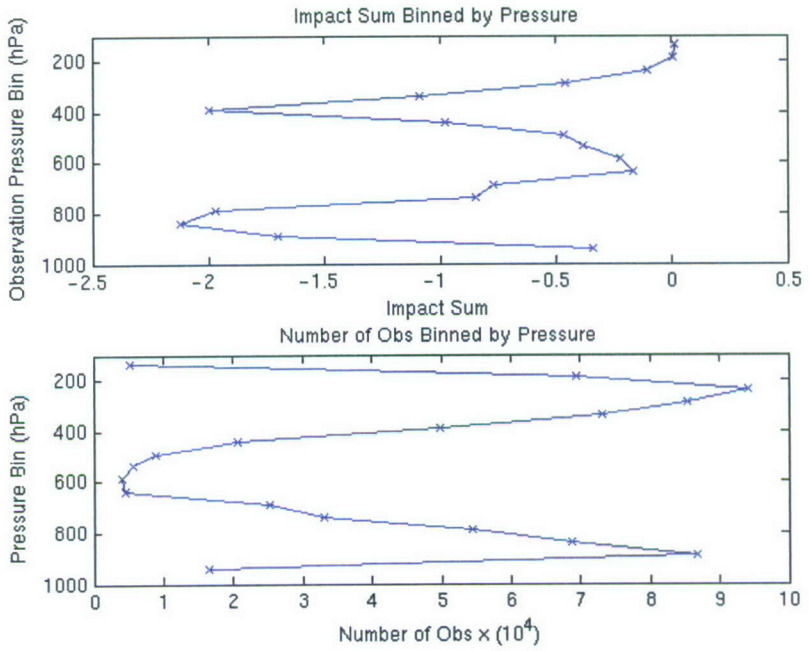


**Figure 5:** Observed AMV pressure vs. summed observation impact (top panel) and number of observations (lower panel). Peak impacts occur at about 850 hPa and 400 hPa.

Data assimilation procedures create analyses of atmospheric fields by blending information from the background with new observations. An observation's influence on the analysis is determined largely by the ratio of the assumed error of that observation with the assumed error of the background (a short-range model forecasts) at the observation location. Observations that are believed to be more accurate (e.g., smaller observation error) receive more weight than do less accurate observations. In NAVDAS, the assumed error of wind observations is a function of pressure level (see Figure 7). The true observation and background errors are unknown, so a large fraction of observations consequently produce either too much or too little influence on the analysis.

It is useful to examine the correlation of observation impact with the assumed observation and background errors. Figure 6 shows the summed AMV observation impact plotted with the ratio of the assumed observation error $\sigma_{ob}$ and the assumed background error $\sigma_{bk}$. This ratio is $\lambda_{ob} = \frac{\sigma_{ob}}{\sigma_{bk}}$. The AMV observation impact is most beneficial when $\lambda_{ob}$ = 1.5, a ratio of AMV observation error and NOGAPS background error that is close to "optimal" for the current NAVDAS. Why this is so needs to be explored further. Slightly more observations have $\lambda_{ob}$ =1.4, but these observations have less beneficial impact, even though they are assumed to be more accurate relative to the background. This suggests that the observation error for these AMVs may be underestimated or over-estimated. There are also larger numbers of observations for which $\lambda_{ob} \geq$ 1.6, but again their summed impact is again less beneficial than those for $\lambda_{ob}$ = 1.5. As observation error increases, they receive less weight in the data assimilation

procedure, and their impacts should become smaller. Note that $\sigma_{ob}$ applies to the superobbed AMV observations not the individual AMVs.

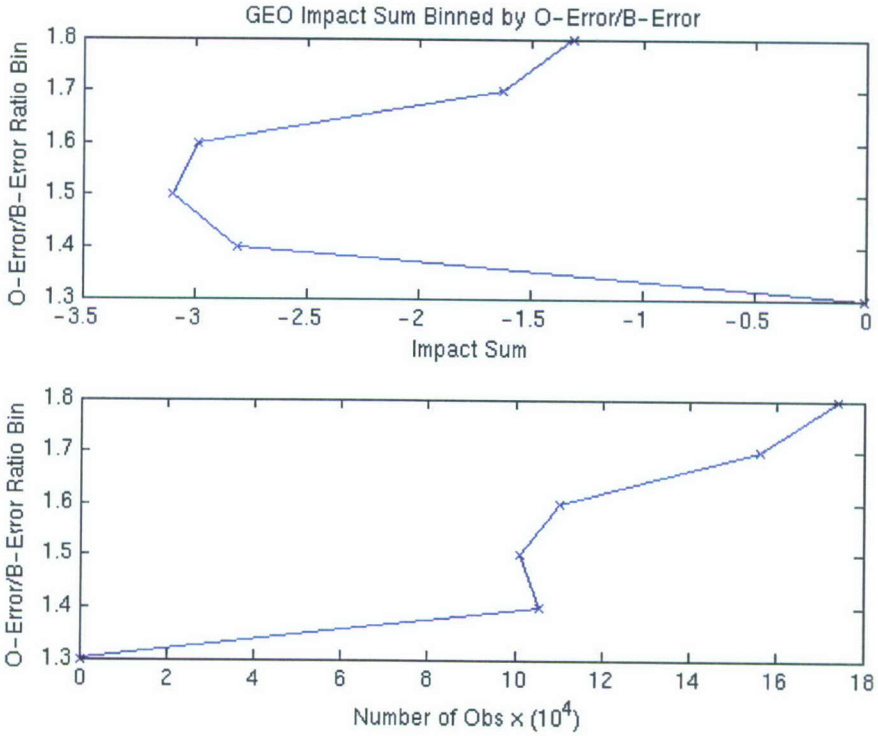


**Figure 6:** Ratio of assumed AMV observation error / background error vs. summed observation impact (top panel) and number of observations (lower panel). Observations with the most beneficial impact have observation errors that are 1.5 times as the value of the background error.

### 3. Observation and Background Error Ratio Experiment (Exp 1)

In this section we describe an experiment to test the hypothesis that NOGAPS forecasts will be improved if AMV observation errors are adjusted to impose a ratio of $\lambda_{ob}$ = 1.5. The current operational AMV observation errors are shown as red circles in Figure 7 as a function of pressure. The minimum observation error is 2.8 $ms^{-1}$ at the low levels and increases to a maximum of 5.2 $ms^{-1}$ above 300 hPa. The green circles represent the observation errors that result when $\lambda_{ob}$ = 1.5, retaining the operational values of the

assumed background wind error. At most pressure levels, this change implies small reductions (< 1 $ms^{-1}$) of assumed AMV observation error. However, there are small increases in observation error near 400 hPa and from about 800-950 hPa.

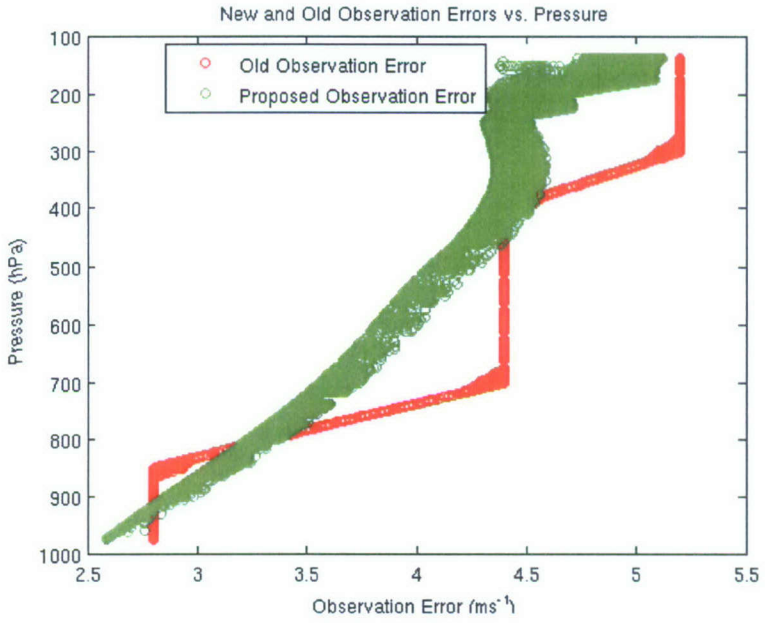


**Figure 7**: AMV observation errors as a function of pressure. The red circles are the operational NRL AMV observation errors. The green observation errors are the observation errors that result if the observation error equals 1.5 times the background error.

In this experiment two data assimilation and forecast cycles are run, daily, from 1 April to 30 April 2007. We use all NOGAPS operational observations, except for the substitution of special CIMSS AMVs that include an "expected error quality indicator" (see Section 4). The control forecast uses the operational AMV observation errors. The experimental forecast uses the exact same set of observations as the control run, but changes the assumed AMV observation error so that $\lambda_{ob} = 1.5$. This change is imposed

for all AMVs in the global domain, at all pressure levels. The forecast impact results of this experiment are described in Section 7.

## 4. AMV Quality Indicators and Expected Error Estimates

As described above, specifying the appropriate observation error is critical to data assimilation and forecast quality. Specifying it correctly for AMVs, however, is relatively difficult. The derived nature of the product using multiple satellite images, along with assumptions about background winds provided by forecast models makes estimating the true error of these observations difficult. It has also been shown that AMV observation errors are spatially correlated, and this complexity is not handled well by current variational data assimilation procedures.

Traditionally, AMV producers have not estimated the observation error directly; Instead, they assign normalized quality indicators to assess whether a particular AMV is "good" or not. Operational AMV producers generate two objective methods: the recursive filter (RF) method (Velden et al 1998) and the automatic quality indicator (QI) method (Holmlund 1998). Both techniques assign a normalized indicator that measures the vector's fit to its neighbors, consistency, and fit to a background model (Velden et al 2005).

Recently, CIMSS has been experimenting with a quality indicator derived by LeMarshall et al (2004). This indicator, called the "expected error" (EE), linearly regresses the predictors that make up the QI along with additional vector and model information against co-located AMV – rawinsonde differences. A list of the regression components and values for GOES-12 AMVs for various channels is provided in Table 1.

| Predictor | IR | Visible | Water-Vapor | Shortwave IR |
|---|---|---|---|---|
| Constant | 10.1 | 2.92 | 9.33 | 8.85 |
| QI Speed Test | -0.180 | -2.02 | -0.366 | 1.86 |
| QI Direction Test | -0.36 | -1.83 | -0.224 | 1.72 |
| QI Vector Test | -0.99 | 1.88 | -0.739 | -2.66 |
| QI Buddy Test | -1.83 | -1.72 | -1.72 | -2.02 |
| QI Forecast Test | -3.02 | -1.90 | -3.56 | -1.45 |
| AMV Speed | 0.092 | 0.183 | 0.101 | 0.06 |
| AMV Pressure | $-3.14\times10^{-3}$ | $3.01\times10^{-3}$ | $-9.28\times10^{-4}$ | $-5.5\times10^{-3}$ |
| Model Wind Shear | 0.405 | 0.012 | 0.022 | 0.091 |
| Model Temp. Gradient | 0.030 | -0.025 | 0.0290 | 0.031 |

**Table 1:** Expected Error linear regression coefficients for Northern Hemisphere GOES-12 Infrared, visible, water vapor, and shortwave IR AMVs.

Figure 8 and Figure 9 show two measures of the EE's skill and highlight the two ways it will be used in this study. Infrared AMVs from GOES-12 are co-located with rawinsondes. The results shown below were generated from AMVs collocated with rawinsondes from September – November 2007. The EE's performance varies little from month to month. Box-and-whisker plots of AMV-rawinsonde distributions grouped by a central expected error bin value (i.e. a bin of 6 $ms^{-1}$ contains AMVs that have expected errors between 5.5 $ms^{-1}$ and 6.4 $ms^{-1}$) are shown in Figure 8. The 1-1 line is shown for comparison. If the EE were a perfect predictor all of the AMVs would fall on this line.

Although many of the AMVs do not, most of the mean and median values of the distributions do fall fairly close. The mean and medians of the AMV – rawinsonde difference distributions generally increase with increasing EE. Analyzing the EE in this way suggests that it has skill at estimating AMV error compared to rawinsonde error. Even if the EE were a perfect correlative measure of AMV – rawinsonde differences, however, it would only be an approximation of the true AMV observation error. The EE does not take into account rawinsonde measurement or representative-ness error between rawinsondes and AMVs, nor does it account for errors introduced by imprecise collocations.

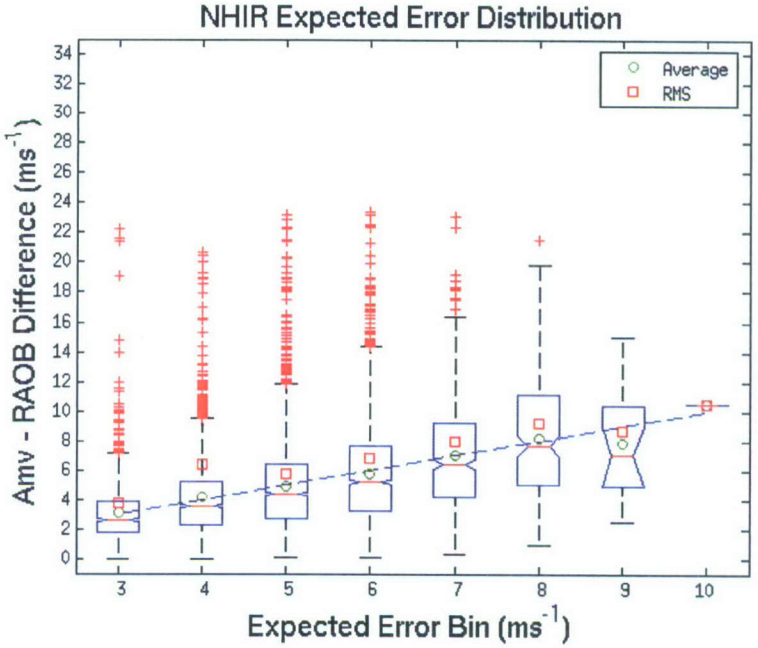


**Figure 8:** Box and whisker plots showing the distributions of actual AMV –RAOB (rawinsonde) differences as binned by a central expected error. The lower line of the box, the red line in the middle of the box, and the top line of the box represent the lower quartile, the median, and the upper-quartile of the distributions, respectively. The red crosses are outliers. The average (green circle) and rms (red square) values for each distribution are also shown. A 1-1 dotted line is shown for comparison.

As discussed in Section 3, estimating the observation error is important. But the EE can also be used to decide whether a given observation should be assimilated or not. Figure 9 bins the AMV – rawinsonde differences by the maximum EE rather than a central value as in Figure 8. The 1-1 line is also shown. This figure shows that errors decrease as the maximum threshold decreases. On average, however, they do not decrease by an appreciable amount until the EE thresholds drop below about 7 $ms^{-1}$. Most of the EEs are below this value (see Figure 10). As the threshold gets lower, the error distributions move toward lower errors as well, reflecting the EEs skill at thresholding out bad AMVs.

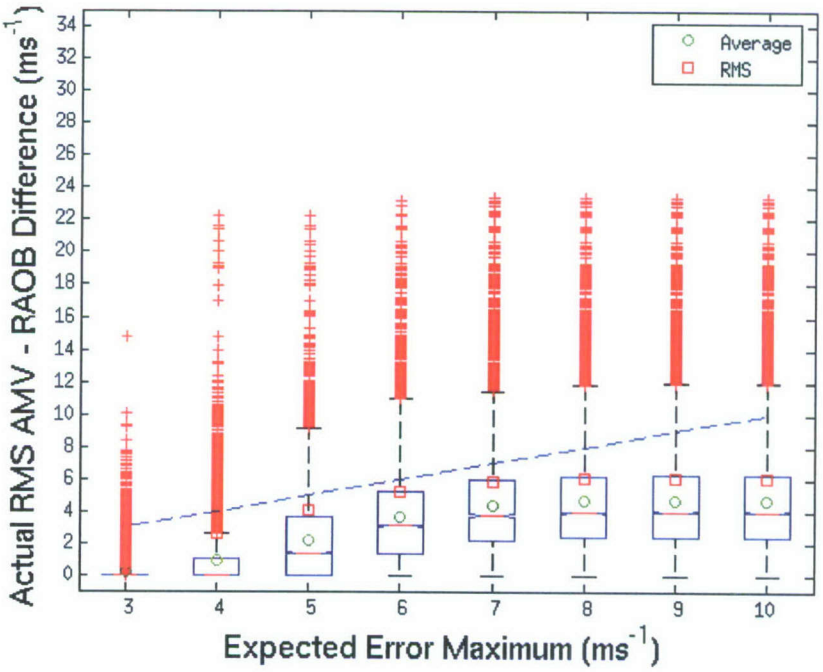


**Figure 9**: As in Figure 8, except the box plots represent the AMVs that have the maximum expected error value shown in the x-axis. As the expected error maximum threshold decreases, the errors generally decrease, particularly when the threshold value decreases below about 7 $ms^{-1}$.

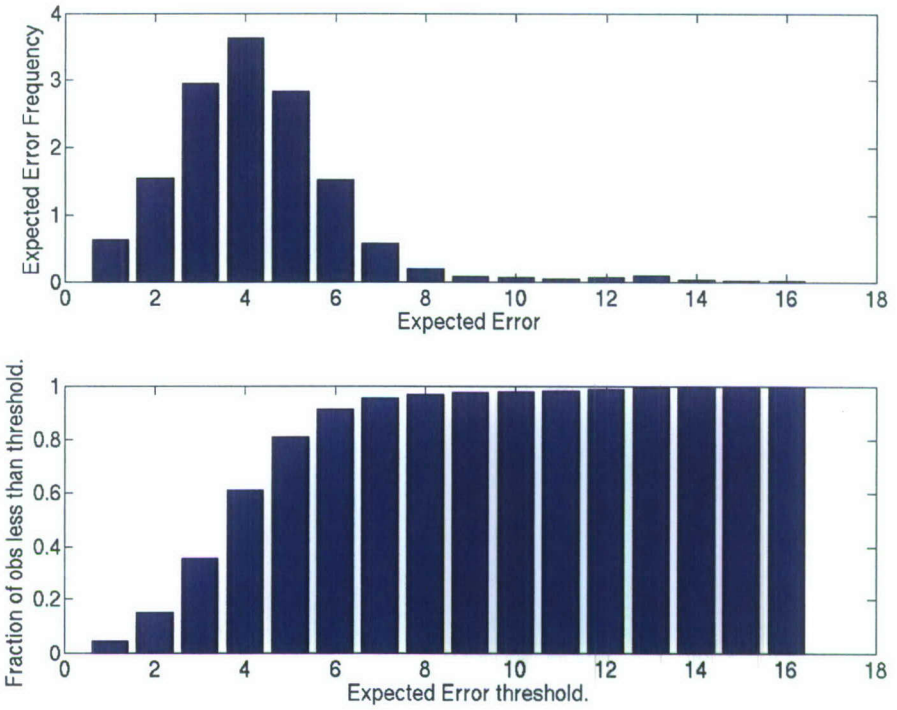


**Figure 10:** (Top plot) Expected Error histograms (x $10^4$) for GOES-E, GOES-W and Metosat-9 AMVs for April 1-2 and April 15-16, 2007. (Bottom plot) Cumulative distribution for the same dataset.

The results shown in Figure 8 and Figure 9 are confined to only those AMVs that are co-located with rawinsondes. AMVs not necessarily matched with rawinsondes are shown in Figure 10: a histogram and cumulative probability distribution of the EE from four days of AMVs during the month of April, 2007. The average EE is about 4 $ms^{-1}$ and most of the EEs are below 8 $ms^{-1}$. These results are reasonably consistent with the results for AMVs co-located with rawinsondes.

## 5. EE Threshold Experiment (Exp 2)

The AMV EE information can be used to design additional data assimilation and forecast experiments. In Experiment 2 we use the EE to define AMV quality threshold values and withhold poor-quality AMVs from being assimilated. If the threshold value is set too tight, then too many AMVs are rejected and the experiment will not have much impact. If the threshold is set too loose, then too few AMVs are rejected, and the analysis may be degraded. Another consideration is that the EE is a function of AMV speed. Faster AMVs should therefore be given a higher EE tolerance. Based on an analysis and tests with NRL's superob procedure, the threshold values in Table 2 were selected For Experiment 2.

| **AMV Speed** | **EE Threshold** |
|---|---|
| Speed < 50 $ms^{-1}$ | EEs > 7.5 $ms^{-1}$ rejected |
| Speed > 50 $ms^{-1}$ | EEs > 15 $ms^{-1}$ rejected |

**Table 2:** EE Thresholds used in Experiment 2

In this experiment, the control forecasts use operational quality control procedures and observation error values. The EE threshold forecasts use the values in Table 2 to remove selected AMVs before the assimilation procedure. The forecast impact results of this experiment are described in Section 7.

These EE thresholds were applied to a special set of CIMSS AMVs from the period of 1 – 31 April 2007, which include the expected error information. Note that the CIMSS winds are only a subset of all AMVs in the global domain. How much of a subset? An

example of typical AMV numbers is shown in Table 3. The table shows a sample of AMV superobs generated from AMVs from each regional data provider and compares them to superobs generated from AMVs produced at CIMSS. Although the counts are from July, 2007, these numbers are not likely to vary appreciably from month to month. With the exception of Meteosat-9, CIMSS produces fewer AMVs than the other producers. This difference may be to due to quality control differences between the producers. As only the CIMSS AMVs are affected by using the expected error, the numbers in the CIMSS column represent the number of observations that will be affected by the thresholding and the subsequently described expected error-observation error experiment. Keep in mind, however, that the geographic distribution between CIMSS and the other producers is nearly identical. Thus, modifying only the CIMSS AMVs should not have a geographic bias.

| | NESDIS | CIMSS |
|---|---|---|
| GOES | 350850 | 313884 |
| | EUMETSAT | CIMSS |
| Met-7 | 120414 | 76754 |
| | EUMETSAT | CIMSS |
| Met-9 | 148154 | 355134 |
| | JMA | CIMSS |
| MTSAT | 119546 | 102068 |
| | Others | CIMSS |
| Total | 738964 | 847840 |

**Table 3:** Number of AMV superobs (all channels) from July 2007 generated from AMVs by each satellite from CIMSS and the respective national producer. Although CIMSS AMVs represent the majority of total AMVs, the modifications in experiment 2 and 3 are not made to all of the available AMVs.

## 6. EE and Observation Error Experiment (Exp 3)

In Experiment 3, all of the observations are assimilated as in the control, but the EE replaces the operational observation error for all CIMSS AMVs. Figure 11 is a scatter plot of operational AMV observation error versus the EE. For most AMVs the EE is somewhat larger than the operational error, so that the observation will receive somewhat less weight in the analysis. This is particularly true for AMVs with higher speeds that generally have higher EE. Some AMVs, however, have particularly low EE. These low EE AMVs are generally slow in speed, and in the low levels.

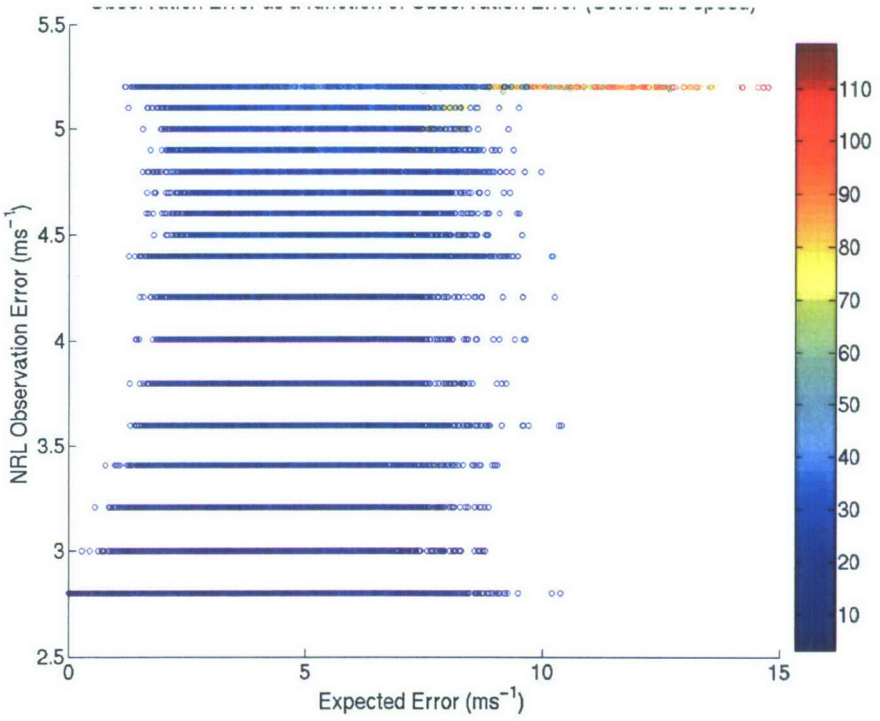


**Figure 11:** Scatter plot of operational AMV observation error and "expected error" for AMVs used in Experiment 3. Color scale corresponds to AMV speed.

| Experiment | Description |
|---|---|
| 1. Observation and Background Error Ratio Experiment | Observation errors for all AMVs are modified so that the observation/background error ratio is 1.5 |
| 2. Expected Error Quality Threshold Experiment | CIMSS-produced AMVs are rejected if their expected errors are above set thresholds |
| 3. Expected Error as Observation Error Experiment | Observation errors for CIMSS-produced AMVs are set to expected error. |

**Table 4**: Summary of data impact experiments.

## 7. Experiment Results

This section describes the forecast impact results of Experiments 1, 2, and 3 that are configured as in Table 4.

### 7.1 Experiment 1- AMV Observation and Background Error Ratio

Modifying the AMV observation errors so $\lambda_{ob} = 1.5$ produced neutral to slightly positive impact. Figure 12 shows the 500-hPa anomaly correlations for the Northern Hemisphere, Southern Hemisphere, and the Tropics. None of the anomaly correlation differences are statistically significant. On average, the Northern Hemisphere and Southern Hemisphere experiments were slightly positive (compared to the control) for long forecast times while the tropical result was slightly negative in terms of 500-hPa anomaly correlation.

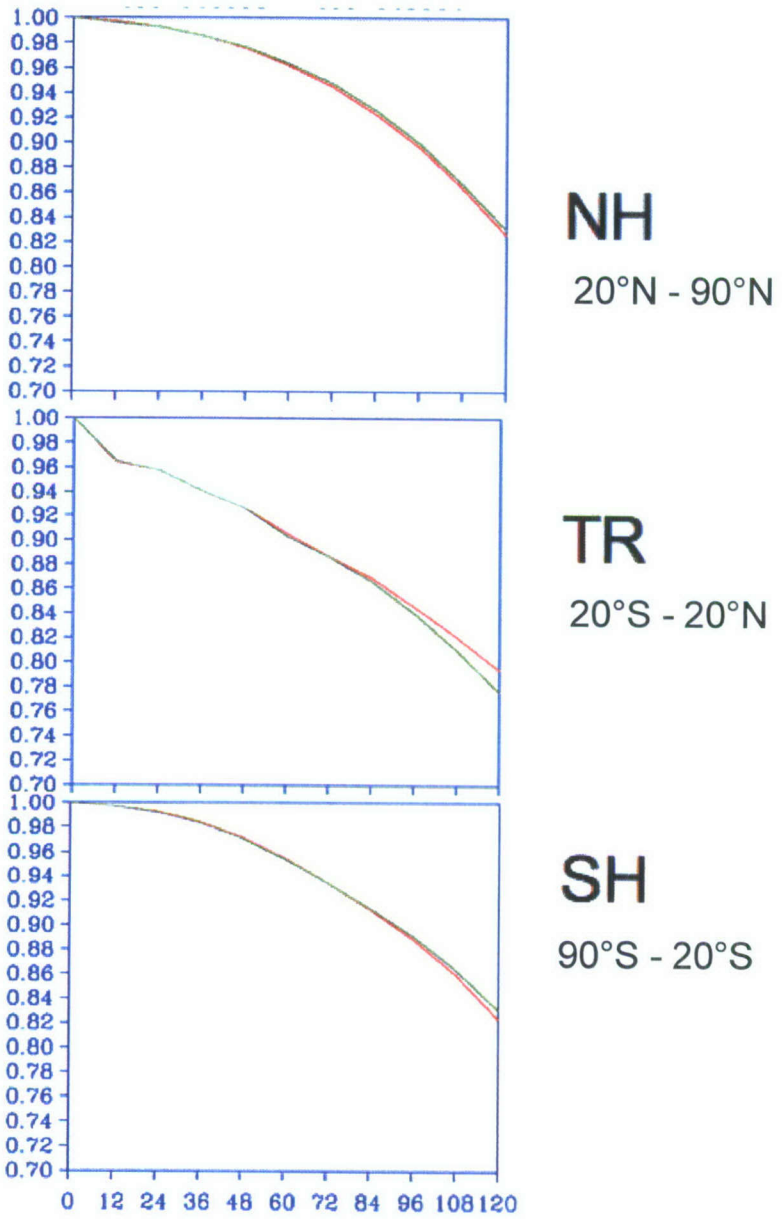


**Figure 12:** Experiment #1 anomaly correlation of 500 hPa height. Northern Hemisphere (top), tropics (middle) and SH (lower). Control forecasts (red) and forecasts with modified observation error (green). The anomaly correlation differences are not statistically significant, although forecast skill is slightly improved outside the tropics with the modified observation error.

| Level | 24-hour | 48-hour | 72-hour | 96-hour | 120-hour |
|---|---|---|---|---|---|
| 850 hPa | 0.015 | **0.037** | **0.046** | **0.056** | **0.052** |
| 700 hPa | **-0.028** | -0.011 | 0.007 | 0.017 | 0.008 |
| 500 hPa | **-0.057** | **-0.053** | -0.042 | -0.021 | -0.04 |
| 250 hPa | **-0.108** | **-0.147** | **-0.132** | -0.117 | -0.045 |

**Table 5:** Differences of root mean square (RMS) wind vector forecast error between the control and modified observation error forecasts in Experiment 1, for the tropics (20°S-20°N). Positive numbers indicate that forecasts with modified observation error have lower forecast error. Differences in bold are statistically significant with at least 90% confidence.

Experiment 1, however, did produce statistically significant results in terms of root mean square wind forecast error differences (

Table 5), at least in the tropical band from 20°S to 20°N. In

Table 5, positive numbers indicate that the RMS forecast error of the modified observation error forecasts is lower than in the control forecasts. As seen in

Table 5, the forecast results differ substantially by level. In general, forecast errors were reduced below 700 hPa, and increased to some extent above 500 hPa by changing the observation error. As forecast length increases, the forecasts with modified observation errors become somewhat more skillful (or less unskillful), although these differences are not statistically significant. Why is the tropical forecast impact different than the extra-tropical forecast impact in this experiment? We might hypothesize that wind observations impact the tropics more than the extra-tropics. Another clue may be seen in Figure 13. This plot shows the same quantities as Figure 6, except for the Tropics

(20°N - 20°S). When the entire global domain is considered, the optimal ratio of observation error to background error appears to be about 1.5. However, for the tropics, the ratio appears closer to 1.4, suggesting that the optimal ratio of observation error to background error might be defined as a function of latitude as well as pressure.

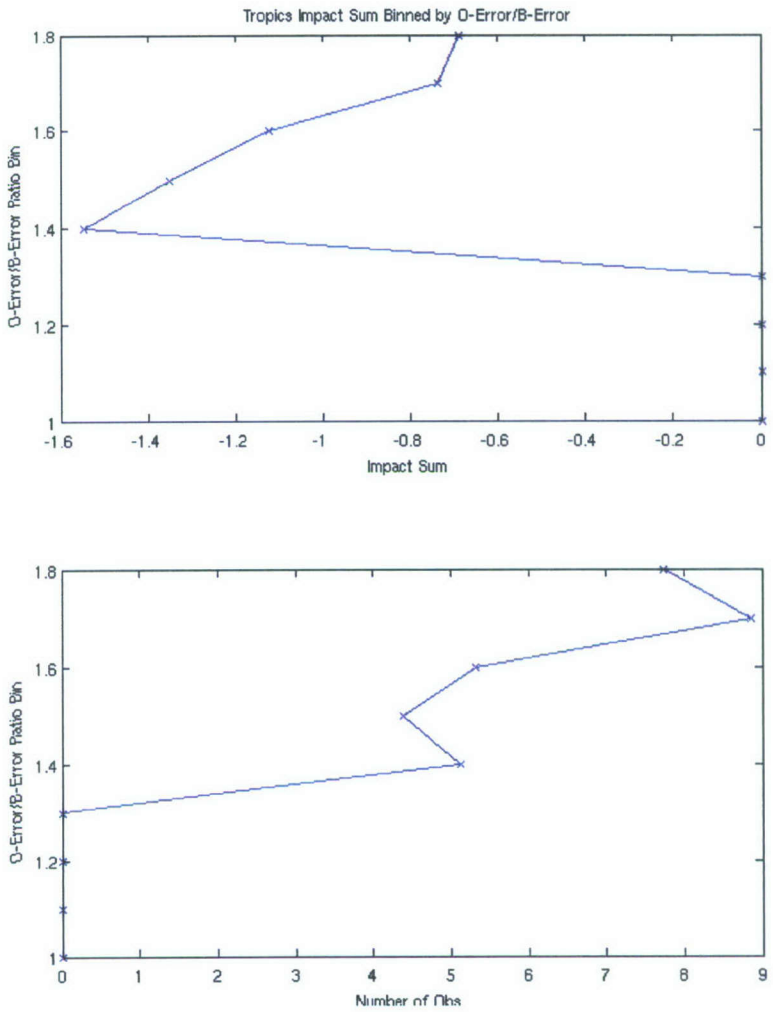


**Figure 13:** As in Figure 6 except for the tropics (20°N through 20°S). The maximum forecast error reduction occurs when the AMV observation error is 1.4 times as large as the background error.

### 7.2 Experiments 2 and 3- EE Threshold and Observation Error Experiments

Results from the EE in Experiments 2 and 3 are essentially neutral in terms of forecast skill. Figure 14 and Figure 17 show the 500-hPa height anomaly correlations results for these two experiments, in which the control forecasts and EE forecasts are not statistically different. The EE threshold experiment (Figure 14) shows a slightly stronger forecast impact than the EE-observation error experiment (Figure 17).

At forecast times longer than about 84hr, the EE-threshold Southern Hemisphere height anomaly correlation is slightly better at 500-hPa and 1000-hPa (not shown). The Northern Hemisphere control forecasts are slightly better than the EE-threshold forecasts.

A time series for Northern and Southern Hemisphere 120-hr rms forecast errors of 250 hpa heights in Experiment 2 is shown in Figure 15. The EE-threshold forecasts have a lower mean RMS error than the control forecasts in the Southern Hemisphere (0.670 m lower) and a slightly higher mean RMS error than the control in the Northern Hemisphere (0.636 m higher). Differences in the Northern Hemisphere wind field (not shown) are also worse (but not significantly worse) than the control. The 120-hr tropical wind vector error time series (Figure 16) also shows the control forecast being slightly better than the experiment (0.073 $ms^{-1}$). These differences are consistent with the fact that changing the AMV assimilation procedure causes greater differences in the Southern Hemisphere, where AMVs comprise a relatively larger fraction of the total available observations.

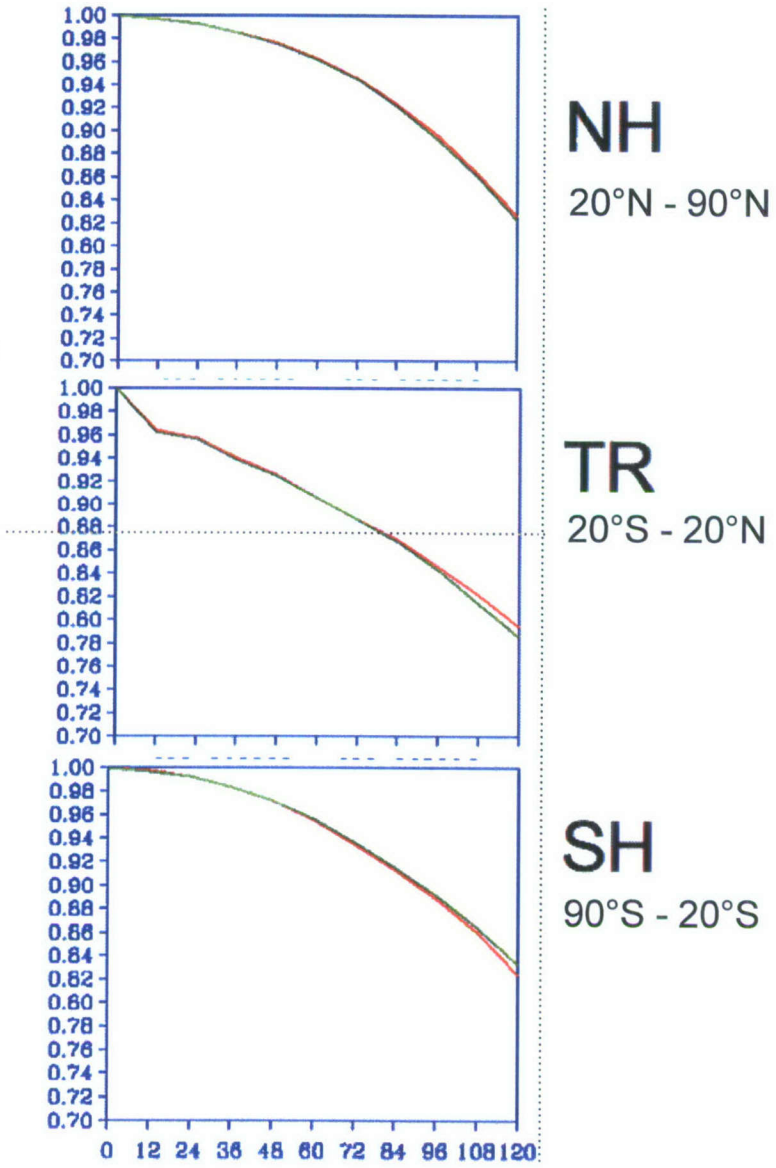


**Figure 14:** Experiment #2 anomaly correlation of 500 hPa height. Northern Hemisphere (top), tropics (middle), and SH (lower). Control forecasts (red) and EE-threshold forecasts (green). The anomaly correlation differences are not statistically different, although the southern hemisphere forecast skill is slightly improved with the EE-threshold.

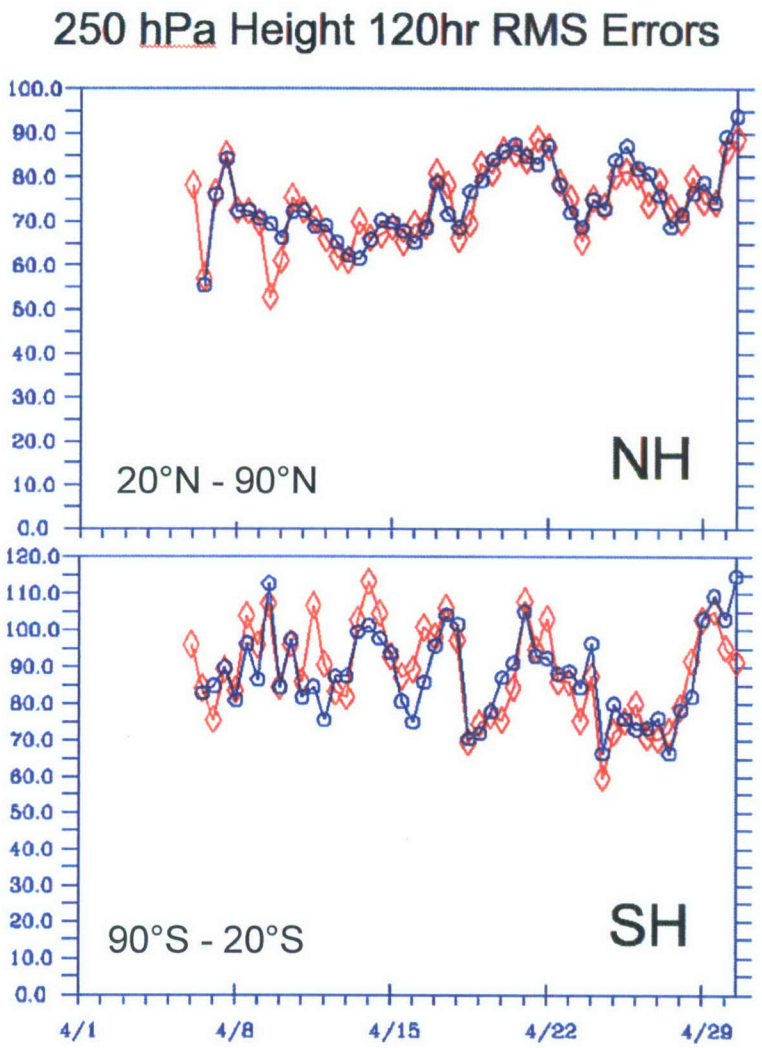


**Figure 15:** Time series of 250 hPa 120-hr RMS height error for the control forecasts (red) and EE-threshold forecasts (blue). The mean error of the EE-threshold forecasts is slightly lower than the mean control error in the Southern Hemisphere and slightly higher in the Northern Hemisphere, although these differences are not statistically significant. The Northern Hemisphere vector RMS (not shown) is consistent with the height error.

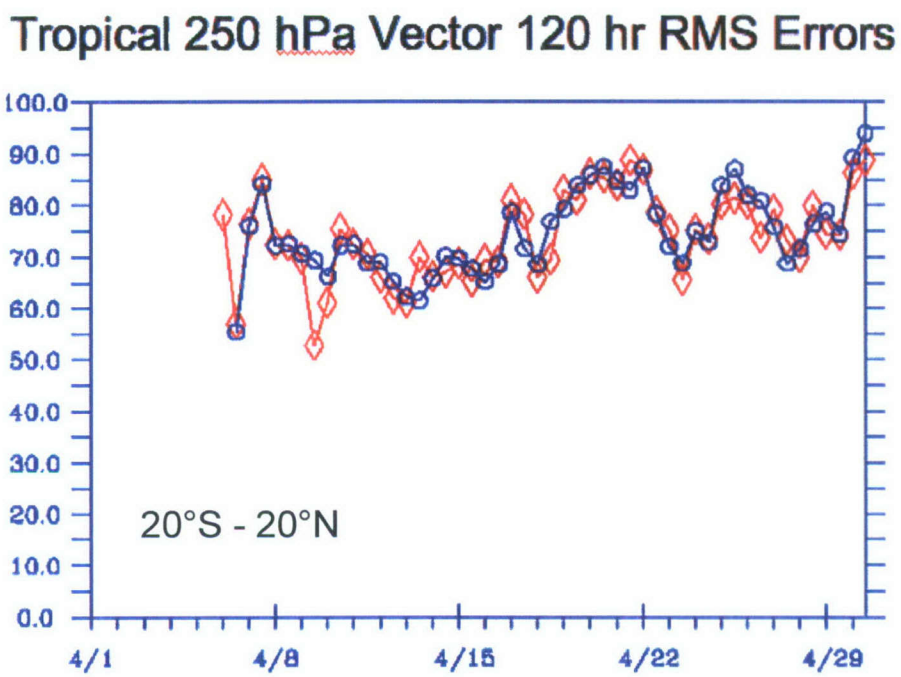


**Figure 16:** Time series of 250 hPa 120-hr RMS height errors for the control forecasts (red) and EE-threshold forecasts (blue). The EE-threshold forecasts are, on average, slightly worse than the control forecasts, although the difference is not statistically significant.

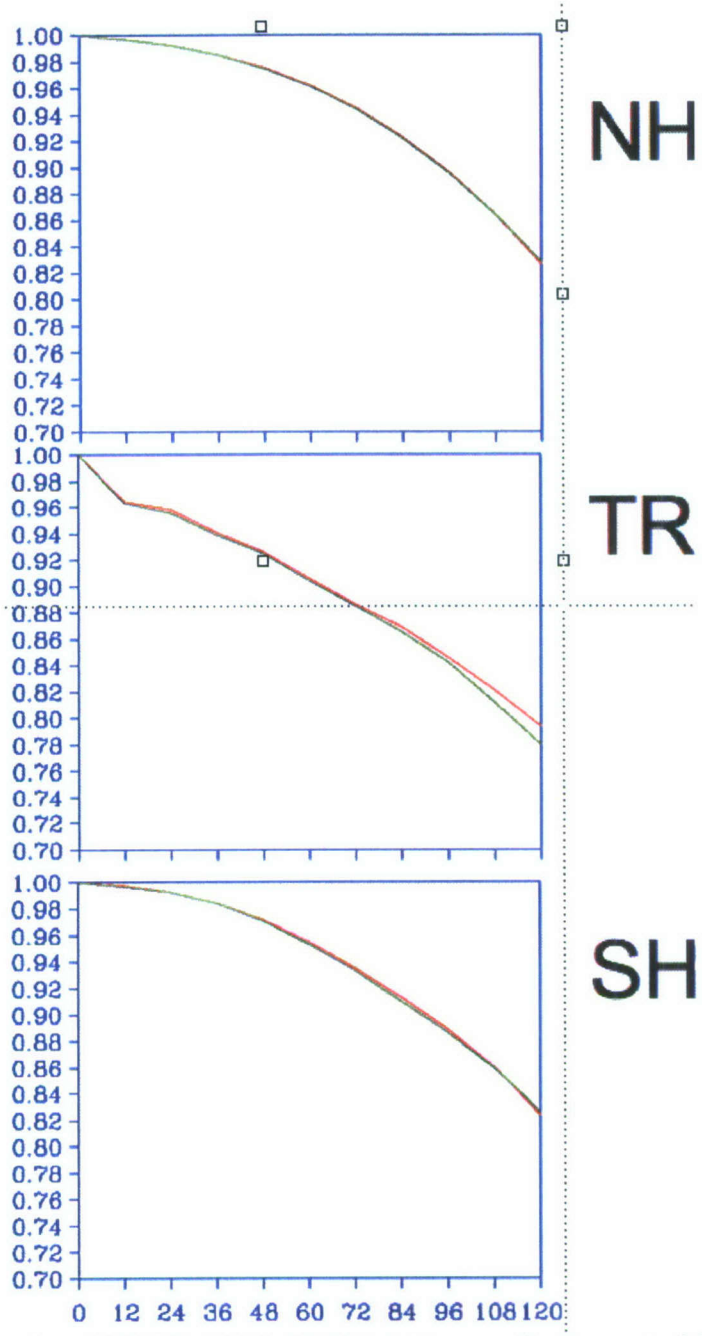


**Figure 17:** Time series of 250 hPa 120-hr RMS height errors for the control forecasts (red) and EE-threshold forecasts (blue). The EE-threshold forecasts are, on average, slightly worse than the control forecasts, although the difference is not statistically significant.

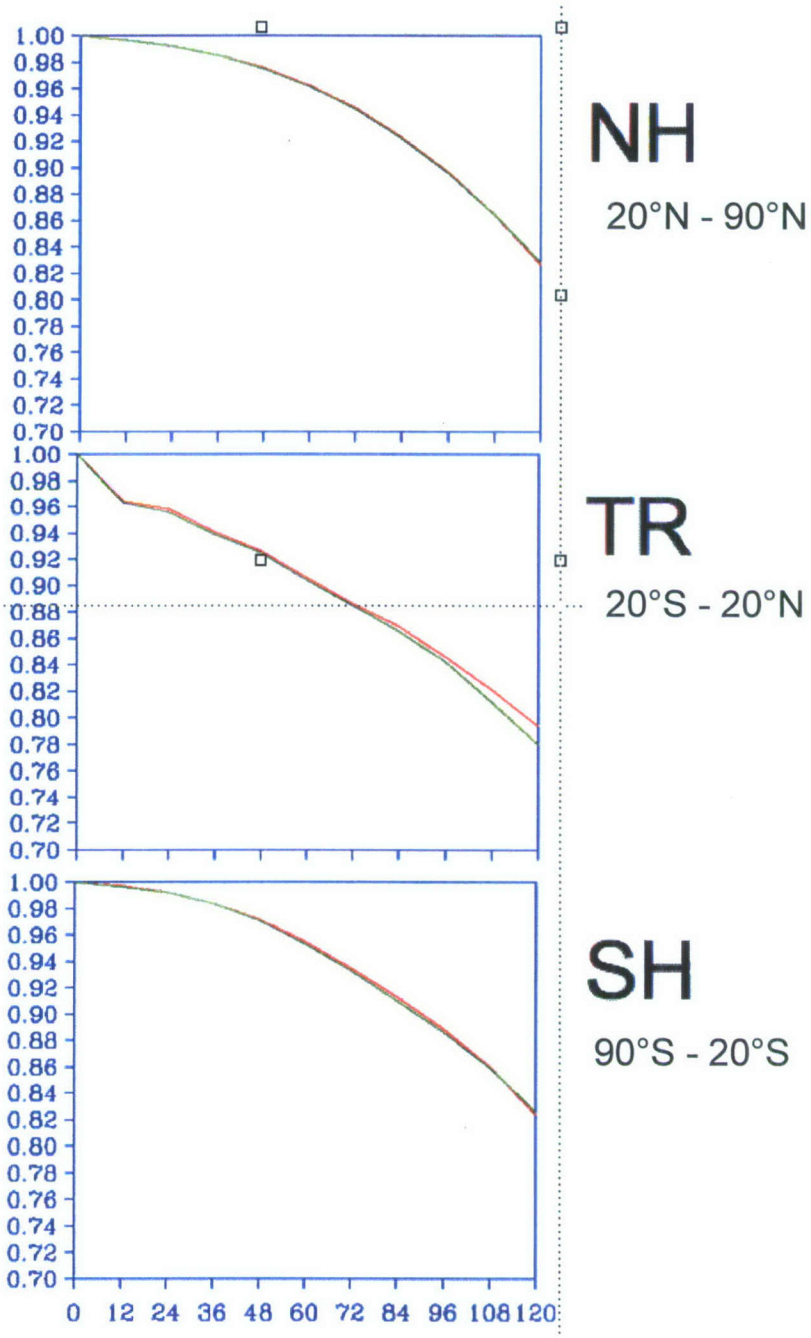


**Figure 18:** Experiment #3 anomaly correlation of 500-hPa height. Northern Hemisphere (top), tropics (middle) and SH (lower). Control forecasts (red) and EE-observation error forecasts (green). The anomaly correlation differences are not statistically different.

In Experiment #3, differences between the EE-observation error forecasts and the control forecasts are relatively small. Figure 19 shows the 250-hPa wind vector RMS forecasts error for the Tropics. The control and EE-observation error forecast differ very little. Similar results are found at other pressure levels and forecast times.

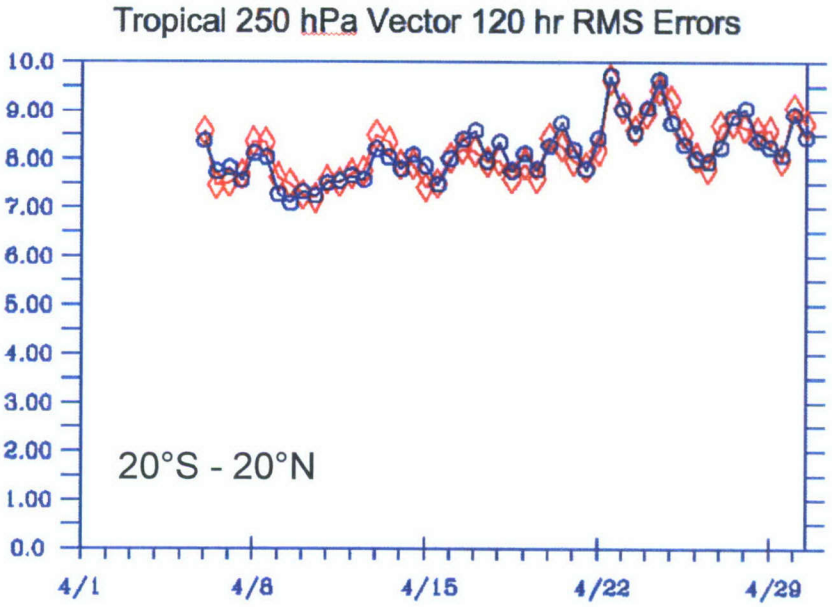


**Figure 19:** Time series of 250 hPa 120-hr RMS height errors for the control forecasts (red) and EE-observation error forecasts (blue). The EE-observation error forecasts are, on average, slightly better than the control forecasts, although the difference is not statistically significant.

## 8. Summary and Future Work

The assimilation of atmospheric motion vectors (AMVs) provides large beneficial impact to NAVDAS analyses and NOGAPS forecast skill. At present, only rawinsonde profiles and AMSU-A radiance observations provide larger contributions to NOGAPS forecast skill, as measured by a global forecast error norm (Langland and Baker 2004). The current assimilation, however, of AMVs (and other observation types) should not be

considered optimal. A major challenge is to provide better estimates of AMV observation error, since this affects the relative weight assigned to the observation versus the background in the data assimilation procedure. Improper specification of observation error can result in degradation of the analysis and poorer forecast quality.

Currently in NAVDAS, the AMV observation error varies only by observation pressure. The observation error is not a function of latitude, longitude, or observed wind speed. This report describes three experiments that test modified assumptions for AMV observation error and quality control. All three experiments produce forecast differences that modestly impact the forecast skill, but with low statistical significance.

***Result 1: Observation and Background Error Ratio Experiment***

The AMV observation error is specified at 1.5 times the background error for all superobs in the global domain. The northern and southern hemisphere extra-tropical 500-hPa height anomaly correlations are slightly better than the control. The tropical 500-hPa height anomaly correlations are slightly worse.

***Result 2: Expected Error Threshold Experiment***

CIMSS-produced AMVs are quality controlled using the EE thresholds described in Table 2. The AMVs produced by the other centers are left unchanged. Forecast impact in the southern hemisphere is slightly better than the control while the northern hemisphere and tropical forecasts are slightly worse.

***Result 3: Expected Error Observation Error Experiment***

Observation errors for the CIMSS AMVs are set to the respective EE values. The modified and control forecasts differ very little.

These results provide some clues and suggest that additional experimentation is required to improve the current assimilation of AMVs in the NAVDAS. Larger forecast improvements may require changes to AMV super-ob procedures or more significant changes to AMV observation errors that affect large fractions of the AMVs. For example, we note that Experiment 1, which modified the observation errors of all of AMVs, also produced the larger forecast impact. In contrast, the two EE experiments affected only those AMVs produced by CIMSS, and thus had relatively smaller forecast impacts. Future experiments might use EE estimates for all AMVs in the global domain.

It might also be useful to introduce a latitude-dependence in the AMV observation error, since AMV observation representativeness may be different in the tropics versus the extra-tropics. The AMV threshold experiment can be modified to make the threshold a linear function of speed rather than using simple cut-off values. A linear threshold would allow additional high-speed AMVs to be assimilated, with tighter restrictions for slower AMVs. The results in Exp 1 clearly indicate some correlation with pressure. The 1.5-modification helped the low level AMV assimilation but hurt the upper levels. This discrepancy needs further investigation. It would also be of interest to calculate the adjoint-based observation impact as a function of the AMV EE. Then, one could better optimize the error threshold to produce the most beneficial selection of AMVs for actual

assimilation. The goal of future experiments is to isolate the fraction of AMVs assimilated in NAVDAS that improve the analysis and forecast quality.

## 9. References


1. Berger, H, Velden, C. and LeMarshall, J. 2006: New quality indicators for GOES derived winds and their potential affect on NWP data impact experiments. In: International Winds Workshop, 8th, Beijing, China, 24-28 April 2006. Proceedings. Available at: http://www.eumetsat.int/Home/Main/Publications/Conference_and_Workshop_Proceedings/SP_1154618862781?l=en

2. Berger H. and Forsythe M. 2004: Satellite Wind Superobbing. UK Met Office Technical Report 451. Available at: http://www.metoffice.gov.uk/research/nwp/publications/papers/technical_reports/index.html

3. Daley R. and E. Barker 2001: NRL Atmospheric Variational Data Assimilation System Source Book

4. Hogan T. F., T. E. Rosmond, and R. L. Pauley, 1999: The Navy Operational Global Atmospheric Prediction System: Recent changes and testing of gravity wave and cumulus parameterization. Preprints, 13th Conf. on Numerical Weather Prediction, Denver, CO, Amer. Meteor. Soc., 60–65.

5. Langland R. and N. Baker 2004: Estimation of observation impact using the NRL atmospheric variational data assimilation adjoint system. *Tellus* **36A,** 189-201

6. Pauley, P. 2003: Superobbing Satellite Winds for NAVDAS. NRL Technical Report

7. Velden, C. S., T. Olander, and S. Wanzong, 1998: The Impact of Multispectral GOES-8 Wind Information on Atlantic Tropical Cyclone Track Forecasts in 1995. Part 1: Dataset Methodology, Description and Case Analysis. Mon. Wea. Rev., 126, 1202-1218.

8. Velden, C., J. Daniels, D. Stettner, D. Santek, J Key, J. Dunion, Holmlund, K G. Dengel, W. Bresky, and P. Menzel, 2005: Recent innovations in deriving tropospheric winds from meteorological satellites. *BAMS*, **86** 205-213.


## 10. Refereed Publications


Langland, R. H., Velden, C., Pauley, P. M., and Berger, H., Impact of Satellite-Derived Rapid-Scan Wind Observations on Numerical Model Forecasts of Hurricane Katrina. Mon.Wea. Rev., under review.